10. SUPPLEMENTARY MATERIAL

10.1. Supplementary Figure Captions

Figure S1. Optimal chemotherapeutic drug concentration for hydrogel drug delivery. (A) Dose response curve of carboplatin and paclitaxel for seeding density of 20K cells in 30 µL heparin-based hydrogel. **(B)** Graph shows the consistency in percent dead cells using 12.5 nM paclitaxel and carboplatin treatments in both microfluidic *in vitro* experiments and 384 well-plates.

Figure S2. Alexa fluor 594® calibration curve. Graph shows the linear regression between dye intensity and dye concentration.

Figure S3. Microfluidics drug delivery experimental procedure.

10.2. Supplementary Methods for Mathematical Modeling

Laplace's equation was used to describe the electric potential field and electrophoretic transport in the system under study.

$$\nabla^2\varphi = 0 \,, \qquad (1)$$

where φ is electric field potential. By simplifying equation (1) in Cartesian coordinates, assuming the blood vessel is long (i.e., 5000 µm) in x-direction (**Fig. 4B**) and the applied electrical field varies in y-direction.

$$\frac{d^2\varphi}{dy^2} = 0 \,, \qquad (2)$$

where y is the transverse coordinate. In dimensionless form, equation (2) becomes,

$$\frac{d^2\hat{\varphi}}{d\hat{y}^2} = 0 \,, \qquad (3)$$

where $\hat{y}$ is dimensionless transverse coordinate, $\frac{y}{H}$. $\hat{\varphi}$ is the dimensionless electrical potential $\frac{\varphi}{\varphi_1}$ where φ_1 is electrical potential at $y = H$ and φ_2 is electrical potential at $y = -H$. Boundary conditions for equation (3) are described mathematically by Dirichlet conditions of known electrical potentials on the vessel walls. Solving equation (3) with these boundary conditions leads to a linear function for the electrical potential within the tumor bounded by two blood vessels:

$$\hat{\varphi} = \frac{\alpha - 1}{2}\hat{y} + \frac{\alpha + 1}{2} \quad , \tag{4}$$

where α is the ratio between electrical potentials on the vessel walls and is a dimensionless parameter, $\frac{\varphi_1}{\varphi_2}$.

For finding the drug concentration profile over time in the tumor extracellular matrix we used molar species continuity equation [1]:

$$\frac{\partial C_D}{\partial t} = -\vec{\nabla}.\vec{N}_D, \tag{5}$$

where C_D is the molar concentration of drug, t is time, $\vec{N}_D$ is the total molar drug flux. Under the assumption of no convection the total molar flux is equal to the summation of contributions due to diffusion and the applied electrical field:

$$\vec{N}_D = -D\vec{\nabla}C_D + zF\mu C_D\vec{\nabla}\varphi, \tag{6}$$

Where D is the drug diffusion coefficient, z is the ionized carboplatin valence, F is Faraday's constant [2], μ is the carboplatin mobility. By combining equations (5), (6):

$$\frac{\partial C_D}{\partial t} = D\nabla^2 C_D - zF\mu\vec{\nabla}.(\vec{\nabla}\varphi) \quad . \qquad (7)$$

Equation (7) was solved computationally using the finite element method in COMSOL Multiphysics® v. 5.4 (COMSOL, Inc., Stockholm, Sweden). The computational domain is the electrophoresis channel (**Fig. 4B**). The diffusion coefficient of macromolecules is calculated using the Stokes-Einstein equation [3]:

$$D_{Dye\_water} = \frac{9.96 \times 10^{-16} T}{\mu_{water} (V_{Dye})^{1/3}},$$

(8)

where V_{Dye} is the fluorescent dye molar volume, T is the solution temperature, and μ_{water} is water viscosity. The effective diffusion coefficient of fluorescent dyes in heparin-based hydrogel is used for estimation of effective diffusion coefficient of drug in extracellular matrix (ECM). Johansson obstruction model [4] for effective diffusion coefficient of gels is used in the current study:

$$D_{effe} = D_{Dye\_water} exp(-0.84\beta^{1.09}), \qquad (9)$$

where β is effective radius defined in equation (10):

$$\beta = (1-\varepsilon)\left(\frac{r_s + r_f}{r_f}\right)^2,$$

(10)

where ε is heparin hydrogel porosity which is 70 percent, r_s fluorescent dye molecular radius, and r_f is heparin hydrogel fiber radius.

Concentration profile of carboplatin in the tumor microenvironment was calculated using a mass transfer model. The uptake of drug into the tumor cells is modeled by an additional term, R_D , in the continuity equation. To describe the transport of carboplatin from the blood vessels into the surrounding cancer cells, the control volume shown in **Fig. 3A**, we use the molar species continuity with reaction term:

$$\frac{\partial C_D}{\partial t} = -\vec{\nabla}.\vec{N}_D + R_D, \tag{11}$$

where R_D describes the uptake of drug by the tumor cells. We assume the drug uptake is governed by first order kinetics,

$$R_D = -\lambda C_D, \tag{12}$$

$$\lambda = \frac{D}{L^2}, \tag{13}$$

where λ is the cellular uptake rate of the drug. By combining equations (6), (11), and (12):

$$\frac{\partial C_D}{\partial t} = D\nabla^2 C_D - zF\mu\vec{\nabla}.(\vec{\nabla}\varphi) - \lambda C_D. \tag{14}$$

Equation (14) is the microscopic equation of carboplatin transport in the tumor assuming that uptake, diffusion, and electrophoresis transport are present. For finding the drug concentration in the steady state condition, the one directional transport, and dimensionless form, equation (14) becomes,

$$\frac{d^2\hat{C}_D}{d\hat{y}^2} - p\frac{d\hat{C}_D}{d\hat{y}} - q\hat{C}_D = 0, \tag{15}$$

where $\hat{C}_D$ is the ratio of the local concentration of carboplatin in the tumor tissue and that in the blood vessel (source), $\frac{C_D}{C_{D0}}$. Boundary conditions for solving ordinary differential equations analytically [5], equation (15), are specified concentrations equal to the concentration of drug in the blood on the blood vessels walls, the boundaries of the system under study:

$$\hat{C}_D(\hat{y} = 1) = 1, \tag{16}$$

$$\hat{C}_D(\hat{y} = -1) = 1, \tag{17}$$

solving equation (15) with these boundary conditions leads to:

$$\hat{C}_D = \frac{sinh(m_2)}{sinh(m_2 - m_1)} e^{m_1 \hat{y}} + \frac{sinh(m_1)}{sinh(m_1 - m_2)} e^{m_2 \hat{y}}, \tag{18}$$

For predicting percent dead cells using the mathematical model, we present the novel physics-based model. The model is based on the fraction of cells killed in the monolayer surrounding one blood vessel. The linear function describing the fraction of cancer cells killed in a monolayer (i.e., neglecting diffusive transport) experiment is detailed in Pascal et al. [6]. Moarefian et al. [7] upgraded a model by adding diffusive and electrophoresis transport. The volumetric average of this function was used to determine the fraction of cells killed over the area of tumor between two blood vessels (drug sources) (**Fig. 3A**).

In the current study, Pascal et al.'s approach for predicting the fraction of tumor cells killed in a monolayer is modified for Cartesian coordinates:

$$f_{kill} = \frac{2.l.w}{V_{Total}} \cdot \int_{H-y_k}^{H} f_{kill}^{M}(C_D(y)) \cdot dy \quad , \tag{19}$$

where H is half the distance between two blood vessels or the height of the control volume (**Fig. 3A**). Where y_k is the killed distance from the center of control volume between two blood vessels to the tumor region surrounding one blood vessel, l is the rectangular control volume length, w is the rectangular control volume width, $f_{kill}^{M}(C_D(y))$ is the fraction of cells killed in a monolayer cytotoxicity experiment. $C_D(y)$ is the local concentration of drug. V_{Total} is the total volume of the rectangular domain surrounding one blood vessel,

$$V_{Total} = \frac{V_{Tumor}}{N_{bloodvessels}} = \frac{V_{Tumor}}{V_{bloodvessels}} \times \frac{V_{bloodvessels}}{N_{bloodvessels}} = \frac{1}{\frac{V_{bloodvessels}}{V_{Tumor}}} \times \frac{V_{bloodvessels}}{N_{bloodvessels}} = \frac{V_{\sin glebloodvessel}}{\frac{V_{bloodvessels}}{V_{Tumor}}} = \frac{V_{\sin glebloodvessel}}{BVF} \tag{20}$$

where V_{Tumor} is the tumor volume, $N_{bloodvessels}$ is the number of all blood vessels in a tumor, BVF is blood vessel fraction, which is the volume of all blood vessels to the tumor volume, and $V_{bloodvessels}$ is the volume of blood vessels in the tumor region, which is the tumor's void volume responsible for drug supply (**Figure 3A**). In this study, BVF is 0.7. By combining (19) and (20), we obtain:

$$f_{kill} = \frac{2BVF}{H} \bullet \int_{H-y_k}^{H} f_{kill}^{M}(C_D(y)) \bullet dy \tag{21}$$

Assuming a linear function describing the fraction of cancer cells killed in a monolayer, the fraction of cells killed in the rectangular case studied is determined by:

$$f_{kill}^{M}(C_D(y)) = f_{kill}^{M}(C_D(H)) \cdot \frac{C_D(y) - C_D(H - y_k)}{C_D(H) - C_D(H - y_k)}, \quad (22)$$

where $C_D(H)$ or C_{D0} is the concentration of drug in the blood vessel (maximum drug concentration and $C_D(H - y_k)$ or C_{Dk} is the concentration of drug at the kill depth (minimum drug concentration). Equation (21) in the dimensionless form:

$$f_{kill} = 2BVF. \int_{1-\hat{y}_k}^{1} f_{kill}^{M}(C_D(\hat{y})).d\hat{y}, \quad (23)$$

where $\hat{y}_k$ is the dimensionless killed distance from the blood vessel wall, $\frac{y_k}{H}$. $\hat{y}$ is dimensionless position $\frac{y}{H}$.

Based on the work of Moarefian et al. [7] in a rectangular coordinate and modifying control volume and boundary conditions, a function for the fraction of cells killed for the rectangular case is obtained using equations (18),(22), and (23):

$$f_{kill} = 2BVF.f_{kill}^{M}(C_{D0}) \frac{m_2 \sinh(m_2)(e^{m_1} - (1 + m_1\hat{y}_k)e^{m_1(1-\hat{y}_k)}) + m_1 \sinh(m_1)(e^{m_2} - (1 + m_2\hat{y}_k)e^{m_2(1-\hat{y}_k)})}{m_1 m_2(\sinh(m_2 - m_1) + \sinh(m_1)e^{m_2(1-\hat{y}_k)} + \sinh(m_2)e^{m_1(1-\hat{y}_k)})}$$

(24)

where m_1 and $m_2$are:

$$m_1 = \frac{p + \sqrt{p^2 + 4q}}{2}, \quad (25)$$

$$m_2 = \frac{p - \sqrt{p^2 + 4q}}{2}, \quad (26)$$

where $p = \frac{zF\mu}{2D}(\varphi_2 - \varphi_1) = Pm_1(1-\alpha)$, $q = \frac{\lambda H^2}{D}$, and $Pm_1 = \frac{zF\mu\varphi_2}{2D}$. The roots of m_1 and m_2 are always real because (q) is always positive. Three non-dimensional numbers relate to the physics of uptake, diffusion, and electrophoresis drug transport. Pm_1 is the ratio between the electric potential and diffusivity, q is the ratio between the uptake rate of the carboplatin and diffusivity, and p relates α the electric potential ratio to carboplatin diffusivity.

Independent variables of the mathematical model described in equation 24 are shown in **Table S1.**

Table S1. Independent variables

Independent variable	Symbol	Value
Carboplatin mobility [8]	$\mu\left((\mathrm{mol}\cdot\mathrm{m})/(\mathrm{N}\cdot\mathrm{s})\right)$	$5.1X10^{-10}$
Carboplatin diffusion coefficient [8]	$D(mm^2/s)$	$6.1X10^{-6}$
Carboplatin bulk density [9]	$\rho(kg/m^3)$	18.01
Cellular uptake rate of carboplatin [10]	$\lambda\,(1/s)$	91.66
Tumor depth	$H(m)$	0.0004
Faraday's constant [2]	$F\,(\mathrm{C/mol})$	$9.65X10^5$
Carboplatin valence [11]	z	2

The dependent variables used for sensitivity analysis of the analytical solution are shown in **Table S2** with their sensitivity range and the optimal values for obtaining the maximum fraction of cells killed.

Table S2. Dependent variables

Dependent variable	Definitions	Sensitivity range	Optimized value (f_{kill} max)
q	$\frac{\lambda H^2}{D}$	0.1-50	14.2
Pm_1	$\frac{zF\mu\varphi_2}{2D}$	0-6	3.47
α	$\frac{\varphi_1}{\varphi_2}$	0.01-100	50.00
φ_2		0-70 mV	43.01 mV

Finally, the correlation between mathematical models and *in vitro* experiments was calculated using RNMSE (Root normalized mean square error) and FB (Fraction of bias) methodologies. Table 3S is the summary of the strong correlation between mathematical models: 1. Ionic drug concentration inside the hydrogel with an applied electric field (Concentration+EF). 2. Ionic drug concentration inside the hydrogel without an applied electric field (Concentration Control). 3. Percentage of dead cells model with an applied electric field (%Cells dead +EF). 4. Fraction of cells killed or percentage of dead cells model without an applied electric field (%Cells dead Control) and their corresponding *in vitro* experiments.

Table S3. Drug delivery models and *in vitro* experiment correlation

	FB Fraction of bias	**RNMSE** Root normalized mean square error
	$\frac{2(C_{exp} - C_{model})}{C_{exp} + C_{model}}$	$\sqrt{\frac{(C_{exp} - C_{model})^2}{C_{exp}\, C_{model}}}$
Ideal Value	0	0
Concentration +EF	-0.006	0.004
Concentration Control	-0.053	0.054
%Cells dead +EF	0.2	0.3
%Cells dead Control	0.02	0.3

SUPPLEMENTARY FIGURES

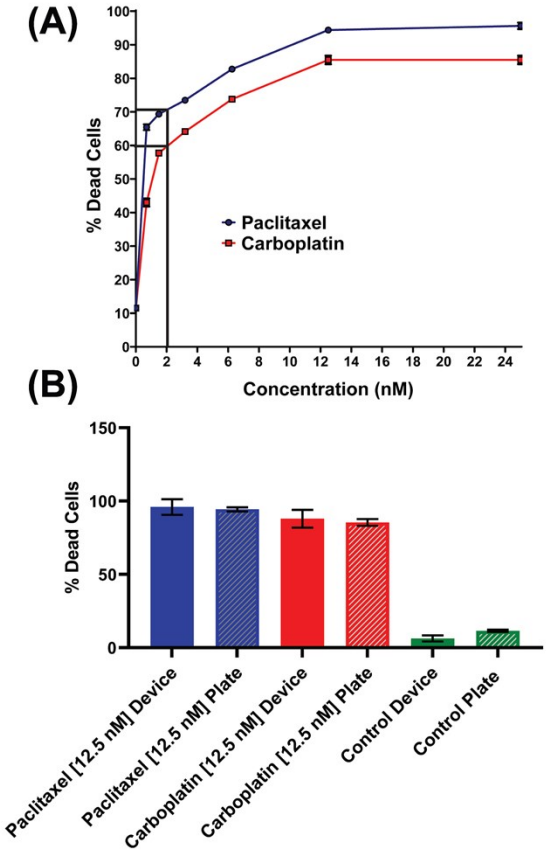

Figure S1.

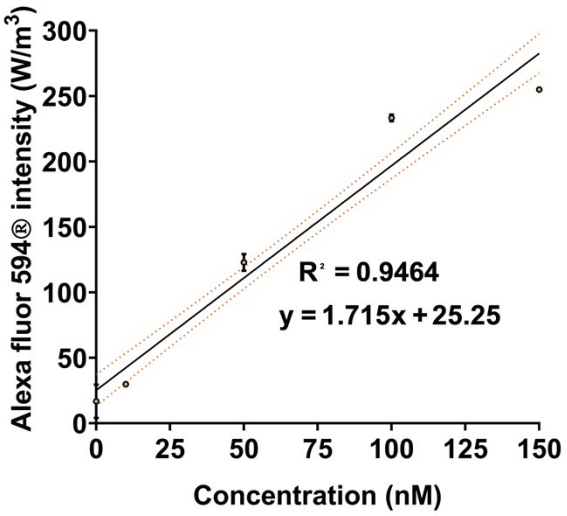

Figure S2.

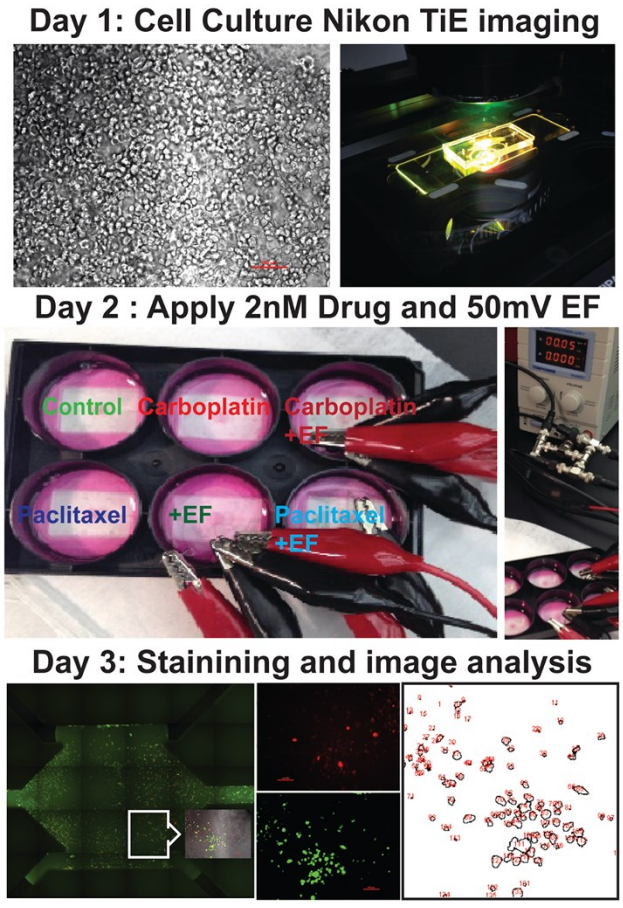

Figure S3.

References

1. Bird, R.B., W.E. Stewart, and E.N. Lightfoot, *Transport phenomena*. 2007: John Wiley & Sons.
2. Probstein, R.F., *Physicochemical hydrodynamics: an introduction*. 2005: John Wiley & Sons.
3. Geankoplis, C.J., *Transport processes and separation process principles:(includes unit operations)*. 2003: Prentice Hall Professional Technical Reference.
4. Johansson, L., C. Elvingson, and J.E. Loefroth, *Diffusion and interaction in gels and solutions. 3. Theoretical results on the obstruction effect.* Macromolecules, 1991. **24**(22): p. 6024-6029.
5. Boyce, W.E., R.C. DiPrima, and D.B. Meade, *Elementary Differential Equations and Boundary Value Problems, Loose-Leaf Print Companion*. 2017: John Wiley & Sons.
6. Pascal, J., et al., *Mechanistic patient-specific predictive correlation of tumor drug response with microenvironment and perfusion measurements.* Proceedings of the National Academy of Sciences, 2013. **110**(35): p. 14266-14271.
7. Moarefian, M. and J.A. Pascal, *Fundamental mathematical model shows that applied electrical field enhances chemotherapy delivery to tumors.* Mathematical biosciences, 2016. **272**: p. 1-5.
8. Pampel, A., D. Michel, and R. Reszka, *Pulsed field gradient MAS-NMR studies of the mobility of carboplatin in cubic liquid-crystalline phases.* Chemical Physics Letters, 2002. **357**(1): p. 131-136.
9. Gust, R. and B. Schnurr, *Investigations on the stability of carboplatin infusion solutions.* Monatshefte für Chemie/Chemical Monthly, 1999. **130**(5): p. 637-644.
10. Binks, S.P. and M. Dobrota, *Kinetics and mechanism of uptake of platinum-based pharmaceuticals by the rat small intestine.* Biochemical Pharmacology, 1990. **40**(6): p. 1329-1336.
11. Di Pasqua, A.J., et al., *Activation of Carboplatin by Carbonate.* Chemical Research in Toxicology, 2006. **19**(1): p. 139-149.